



Experimental and Finite Element Analysis for Evaluating the Fretting Effect on Fatigue Behavior of IMI 834 Titanium Alloy

Sangam Sangral · Maheandera Prabu Paulraj · Jayaprakash Murugesan

Submitted: 21 October 2021 / in revised form: 1 December 2021 / Accepted: 10 January 2022 / Published online: 9 February 2022
© ASM International 2022

Abstract This research article deals with the fatigue behavior of titanium alloy (IMI 834) due to fretting by presenting experimental and finite element analysis (FEA) for the solid bridge-type pad at room temperature. Various stress amplitudes (120–270 MPa) are considered for experimental investigations and the FEA model. Three-dimensional FEA was presented to predict the mechanisms which cause damage, by estimating the performance of stress allocation at various locations like the contact boundaries, crack initiation site, and crack angle. Also, the crack initiation site and crack angle have been calculated by utilizing the results of the proposed model. Using the scanning electron microscope and electron microscopy, the fracture surface and the fretted area are estimated from the tested specimen. From the obtained results, the fatigue life of titanium alloy (IMI 834) due to fretting is gradually decreased for solid bridge-type pad. It may occur because of the elevated stress concentration at the contact boundaries and the higher damage on the surface of the pad. The number of cycles increased with decreasing stress amplitude values for the case of both experimental and FEA model results. The proposed FEA model results are in fine arrangement with experimental end results.

Keywords Fretting · Fatigue · IMI 834 titanium alloy · Finite element analysis · Crack initiation and crack angle · Surface roughness

Introduction

Fretting occurs when two loaded surfaces are in contact with each other and experience the oscillatory motion of a very small amount having relative movement of few microns initiating vibrations or repeated loading [1–3]. Due to these contacts between the components, wear will take place and there is a chance of initiation of crack, which propagates causing failure of the material called fretting fatigue. Fretting degrades the surface quality by the formation of small pits and high surface roughness, which reduces the strength of the material [4, 5]. Many practical examples of this type of failure can be studied in various assemblies, such as dovetail assembly in gas turbine engine [6], body implantation [7], axle-wheel arrangement in the train [8], bolted connections [9], hoisting rope winding [10], thread joint linking oil-well casing pipes [11], and connecting rod arrangement [12].

IMI 834 titanium alloys are elevated temperature alloys established as an alternative for nickel-based superalloys. They are widely used in compressor discs and blades and gas turbine jet engines to enhance fuel efficiency due to their excellent specific strength, extraordinary corrosion, and fatigue resistance [13, 14]. However, the use of these materials is limited to military and aerospace applications due to their excessive price and processing. In these applications, most of the parts are subjected to cyclic loading or vibrations of small amplitude, which leads to very severe damage in the components.

S. Sangral · J. Murugesan (✉)
Department of Metallurgy Engineering and Materials Science,
Indian Institute of Technology Indore, Khandwa Road, Simrol,
Indore, Madhya Pradesh 453552, India
e-mail: jayaprakash@iiti.ac.in

M. P. Paulraj
Department of Ocean Engineering, Indian Institute of
Technology Madras, Chennai, Tamilnadu 600036, India

There exists a wide range of investigation on the effect of fretting on fatigue performance, where investigators have to make an effort to understand the mechanism of failure by considering different fretting fatigue variables, fracture mechanics approach (crack initiation and propagation), damage models approach (critical plane approach, stress invariant approach, fretting-specific parameters and continuum damage mechanics) and 2-D finite element method techniques based on localized stress near the contact boundary. Jayaprakash et al. [15] have determined that in the vicinity or surrounding area of the contact side, the relative slip and tangential stress improved with increasing pad rigidity and determined that the strength due to fretting depends on the combined influence of tangential and compressive stress range. The fatigue strength decreased because of fretting with rising contact stress, which might be because of a slight rise in the tangential force [15–18]. Noraphaiphaksa et al. [19] predicted the relative slip using the FEA model, which was in good arrangement with the experiment, and the crack route was assessed based on the highest tangential stress range criterion. During the cyclic loading, the crack opening occurred due to the compressive bulk stress, referred to as the fretting-contact-stimulated crack opening behavior. Due to fretting, the fatigue lives expected by utilizing the active stress intensity factor range were shorter than those expected by applying the maximum stress intensity factor and were in good arrangement with the experimental end results [19–21]. Walvekar et al. [22] compared the results of an experimental study and a damage model for fretting fatigue. FEA model was suggested to approximate the fretting fatigue life, which was in satisfactory arrangement with the experimental end results. Jayaprakash et al. [23] studied elevated-temperature fatigue performance of titanium alloy due to fretting and concluded that there was a decline in fatigue life because of fretting with rising temperature, which might be due to an escalation in tangential stress coefficient and amplitude of relative slip. FEA model was also designed to assess the stress allocation and relative slip. Quazi Md. Zobaer Shah et al. [24] studied the effect of notch and fretting on bending fatigue using FEM analysis. The analysis was carried out on single-point fretting with double notch and double-point fretting with single notch. It was observed that a single-point fretting with double notches had a higher impact on the fatigue life as compared to the other condition. Xin Li et al. [25] suggested fretting-related damage (FRD) parameter based on the experimental and FEA results. It was verified that the tangential force, Q , had a connection with the impact of fretting. The predicted fatigue life using the damage parameter was in good arrangement with the experiment and can give accurate crack initiation position, crack alignment, and fatigue life prediction results due to fretting. Nadeem Ali

Bhatti [26] and Magd Abdel Wahab [27] adopted different approaches and damage models as mentioned earlier to report the fretting fatigue damage initiation or initiation life. Most of the researchers measured crack opening length varying from 10 microns to 1-mm depth and estimated crack angle between 25 and 50 degrees, since the damage and crack initiate under the contact section at the micro-scale. It was confirmed that accurate modeling for the fretting fatigue problem is still a difficult task. They also implemented standard point and volume averaging methods, which were used and related to the quadrant averaging method to calculate the crack orientation and life of the component. McDiarmid (MD) and Fatemi Socie (FS) damage parameters were utilized to study the variation in all the methods with crack alignment and initiation life. It was noticed that the quadrant averaging method offered more accurate and reasonable results as compared to other methods. Diego Infante-Gracia et al. [28] considered two micro-void distributions to study the effect of heterogeneity for crack initiation in fretting conditions by applying numerical simulations. The numerical results reveal that a crack primarily originates at the micro-voids situated nearer to the contact boundary result in the decline of the anticipated crack initiation life. Guillaume Rousseau et al. [29] proposed a new 3-D model to understand the behavior and service life of the components. The formulation of a nonlinear incremental model was presented to predict the evolution of the intensity factors and the velocity field evolution at the contact boundary and the partial slip zone behavior. At last, the introduction of crack and fatigue life due to fretting was compared with the experimental end results.

Even though several articles were available on fretting fatigue, only a few of them suggested the FEA 3-D model, which can evaluate the crack origination site, crack angle, and fatigue life. A suitable fretting fatigue damage model at present does not exist. It might be due to the complex interaction between the pieces of machinery with a high number of variables involving in fretting fatigue and the damage caused at a microscale level under the contact region, there is a need to come up with a better model or method to understand the fretting fatigue behavior more precisely. At present, only a few research works have been reported on the 3D modeling to study the fretting fatigue mechanism, crack origination site, and crack alignment. So, there is a need for developing some 3D models to assess the fretting fatigue life and damage under fretting with less percentage of error.

In this article, the plain fatigue and fretting fatigue behavior of IMI 834 titanium alloy with the bridge-type flat pad at room temperature have been explored. The findings revealed that the plain fatigue lives were considerably influenced by pad geometry. FEA 3-D model was proposed

based on existing experimental results to identify the mechanism of fretting fatigue, site of crack origination, and crack alignment. Applying the same boundary conditions on both the geometries, then the FEM predicted compared the results with the experimental results. Results were discussed based on the surface roughness, FEM analysis, and scanning electron microscopy.

Theoretical Background

To study various aspects under fretting fatigue conditions, researchers have used different approaches and different damage parameters. These approaches can be classified as critical plane approach, stress-invariant approach, fretting-specific parameters, and CDM approach. According to the critical plane approach for plain fatigue conditions, there are several stress-based parameters under this methodology such as Smith–Watson–Topper (SWT) parameter, the Findley parameter, the McDiarmid parameter, shear stress range parameter as referred to in studies [22, 25, 26, 27, 28, 31 and 32]. However, Findley et al. [30] introduced that the crack originates near the highest shear stress or strain plane, which is prone to initiate damage or failure. This type of method was used by Szolwinski and Farris et al. [31] for fretting fatigue conditions. Further, the Findley parameter (FP) is considered to numerically assess the beginning of a crack in fretting fatigue problems. Based on this parameter, the crack originates on a plane where the combination of both maximum shear stress amplitude and normal stress is maximum [32]. In general, the damage parameters are equated to stress or strain life equation to measure crack initiation location and life. For the present work, only FS parameters are considered to compute crack initiation location and crack angle. The plane, where the damage parameter (FS) achieves its highest value, is designated as the critical plane. Findley parameter is established on stresses and can be stated as:

$$FP = \Delta\tau_{max}/2 + k\sigma_n^{max} \tag{Eq 1}$$

where $\Delta\tau_{max}/2$ and σ_n^{max} are the maximum shear stress amplitude and normal stress on the critical plane. The material constant k acts as an influencing factor to the normal stress component.

Many researchers explained that fretting wear is a complex contact phenomenon. A variety of factors (such as frequency, contact pressure, and relative displacement), including surface roughness, have an influence on the fretting wear process due to which the mechanism is still unclear and the difficulty in simulating fretting wear analysis continues. Some attempts are made to simulate fretting wear to predict the damage mechanism. The Archard equation was adopted by many researchers to

calculate the wear volume loss or wear rate in the component by using the FEA model. The Archard equation can be expressed as [33, 34]:

$$W = K \times s \times P \tag{Eq 2}$$

where W —volume loss, s —sliding distance, P —applied load, and K —wear per unit load per sliding distance.

Equation 2 presents the wear loss based on the local implementation of the Archard wear model. The evolution of contact profile due to fretting wear was simulated using a stress-based wear model proposed by Archard. Based on the stress distribution at different load conditions, the Archard equation is used as shown in Eq 3. This model associates the wear volume with the stress generated by the contact elements, by which the influence of frictional force on fretting wear can be taken into consideration. It has been reported that this model was superior to the commonly used Archard-based wear model when employed to simulate the fretting wear. The modified version of the Archard equation for calculating wear by using numerical analysis can be expressed as [35, 36]:

$$W = K \times S^{C2} \times R^{C3} \tag{Eq 3}$$

where W —volume change, K , $C2$, and $C3$ are equation constants to account for such things as the materials in contact, S —stress created by the contacting pair, and R —number of load repetitions. In this study, the value of K used is 10^{-6} as per the literature in the case of fretting wear and $C2$ is equal to K divided by volume.

One load step corresponding to one fretting cycle is divided into n simulation increments. It is computationally complex to model each fretting cycle. So, according to the cycle jumping technique, the wear rate is unchanged during a given cycle jump. In this way, one load step can model the wear loss generated at n number of fretting cycles based on the stress generated at the contact.

Experimental Procedure

Material, Mechanical Properties, and Specimen

The material utilized for the plain and fretting fatigue test specimens is IMI 834 titanium alloy and for the bridge-type flat contact pad is nickel-based superalloy (Inconel). The chemical composition and mechanical properties of IMI 834 titanium alloy and nickel-based superalloy used are registered in Tables 1 and 2. The dimensions used in this work for the specimen and the contact pad are demonstrated in Fig. 1a and b. The specimen utilized for the test has a gauge length, $GL = 30$ mm, and thickness, $t = 4$ mm, and the contact pad has a contact length of 2 mm with a contact width of 9mm having foot height = 1 mm.

A small piece of IMI 834 titanium alloy was cut longitudinally for optical microscopy. The alloy was polished with emery paper up to 2500 grade followed by diamond polishing and then etched with the solution (2% hydrofluoric acid, 10% nitric acid, and 88% distilled water). Prior to the test, the contact surface of all the specimens and contact pads used were polished up to 2000-grade emery paper and then cleansed with acetone.

Plain Fatigue and Fretting Fatigue Tests

The tests were performed on the servo-hydraulic testing machine at a stress ratio of 0.1 with a frequency of 10 Hz at ambient temperature. The schematic and experimental illustration of fretting fatigue test setup for solid bridge-type flat pad geometries on flat contact configuration is demonstrated in Fig. 2a and b. A constant contact pressure (100 MPa) was employed on the contact pads by using a calibrated proving ring with different cyclic loads at the end of the specimen. The calibrated ring was used to maintain the constant pressure on the pads. During the test, the tangential stress between the specimen and the pad was calculated by fixing strain gauges at the gauge portion of the contact pad.

Surface Roughness, Fracture Surface, and Fretted Area Observation

During fretting, the damage occurred at the surface of the specimen. The surface roughness at the fretted area (the contact region on the specimen which was in contact with the pads) with the bridge-type flat pad was measured by using a coherence scanning interferometer. After the test, the rupture surface of the failed specimen was cleansed using an ultrasonic vibrator for 15 min. in acetone and observed by using a scanning electron microscope. Further,

the fretted area on the smooth surface of the specimen was observed through electron microscopy.

Finite Element Analysis

FEA 3-D model of solid contact pad (bridge-type flat pad) in connection with the smooth surface of the testing specimen has been designed by using ANSYS software to approximate the stress distribution between the contact region and to evaluate the amplitude of relative slip, crack initiation location, and crack angle, as shown in Fig. 3. In this study, the structural analysis was employed and the tetrahedron element type were used in the present model as it gives convincing results in many types of engineering calculations. The simulation of the current investigation was solved as a linear isotropic material model with given material properties. Since material data are crucial to accurate fatigue results, Workbench Simulation readily allows the input of this information to new or existing materials by hand or through load history files. Material properties include density, Young's modulus, Poisson's ratio, and ultimate tensile strength were included in the engineering data file. Materials in the Workbench Simulation material library may include a fatigue stress-life curve populated with data from engineering handbooks. The fatigue tool will then use the information in the stress-life curves for each material in the model when calculating stress distribution, damage, life, etc. The boundary conditions adopted for the present fretting fatigue test were also applied for this analysis based on the experimental study. In the first step, the contact pressure of 100MPa was applied by both the contact pads (top and bottom) to contact the smooth surface of the specimen. In the next step, the load was applied to the specimen by choosing a stress ratio of 0.1 for one second, and the contact between the elements was given as frictional contact, $f=0.8$. FEA 3-D model analysis was performed for all the stress amplitude values used for the fretting fatigue test. Moreover, the present simulations are carried out using an Intel Xenon E5, CPU 3.50 GHz, and 32 GB of RAM. Each run took between 1 and 2 days and thus entire simulation took about four months. The stress distribution, relative slip, frictional stress, wear rate, crack opening site and crack orientation were evaluated in the present study to understand the behavior of the component.

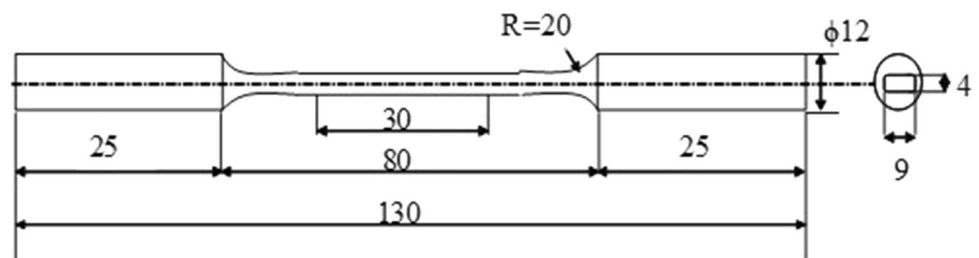
Table 1 The chemical composition of IMI 834 titanium alloy

| Chemical composition (wt. %) | Al | Sn | Zr | Nb | Mo | Si | C | Ti |
|------------------------------|-----|----|-----|-----|-----|------|------|------|
| | 5.8 | 4 | 3.5 | 0.7 | 0.5 | 0.35 | 0.06 | Bal. |

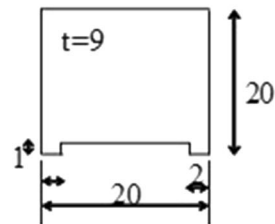
Table 2 The mechanical properties of IMI 834 titanium alloy

| Mechanical properties of IMI 834 titanium alloy | Modulus of elasticity (GPa) | Yield strength (MPa) | Ultimate tensile strength (MPa) | Elongation (%) | Density (g/m ³) | Hardness (Hv) |
|---|-----------------------------|----------------------|---------------------------------|----------------|-----------------------------|---------------|
| | 120 | 935 | 1050 | 12 | 4.55 | 350 |

Fig. 1 (a) Plain fatigue and fretting fatigue test specimen, and (b) bridge-type flat pad. (All dimensions are in mm)



(a) Plain fatigue and fretting fatigue specimen



(b) Bridge type flat pad

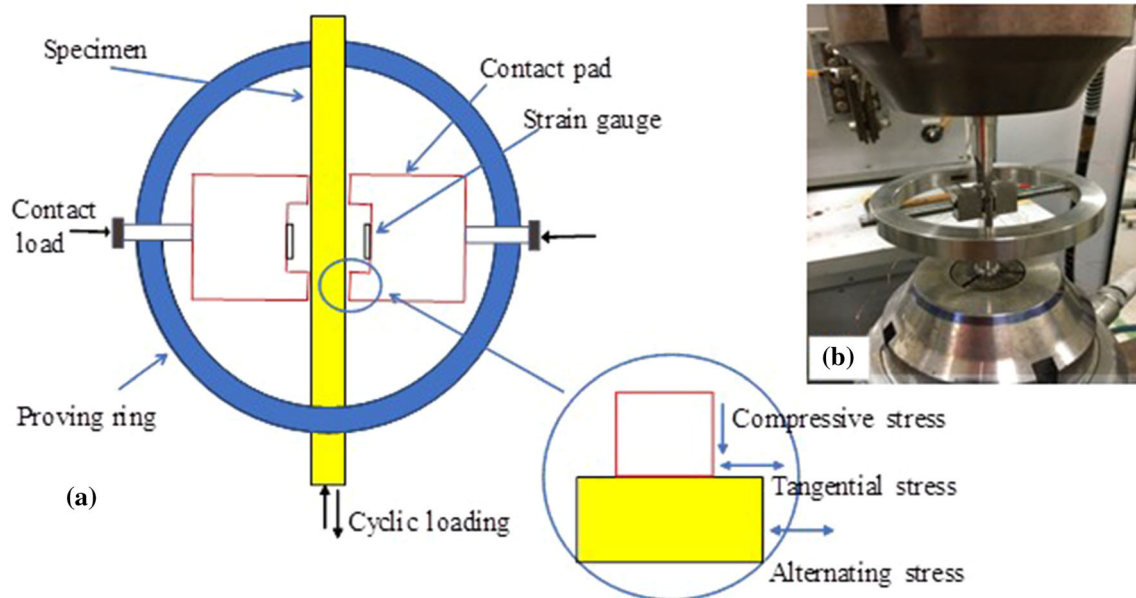


Fig. 2 (a) The schematic illustration of the fretting fatigue test setup, and (b) the experimental setup of the fretting fatigue test

Grid Study for Numerical Analysis

To obtain better accuracy with the reliability of numerical results, the grid test has been carried out by varying the mesh size of elements in all directions (x-direction, y-direction, and z-direction). The stress value varies at the contact region depending on the number of mesh points

used on the contact region, and based on the mesh point factor the life of the material differs. So, the grid study must be done by performing trial-and-error-based analysis with different mesh size models. The grid sensitivity study has been carried out for the case of stress amplitude 270 MPa. Here five different combinations of non-uniform triangular grids have been considered to ensure the

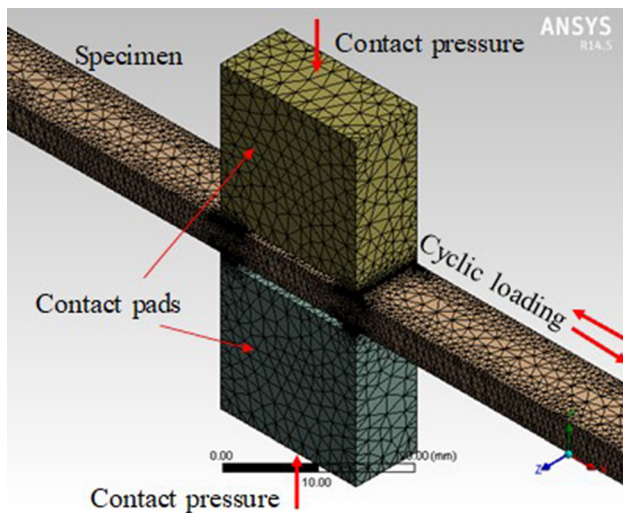


Fig. 3 The FEA 3-D model for fretting fatigue using ANSYS 14.5

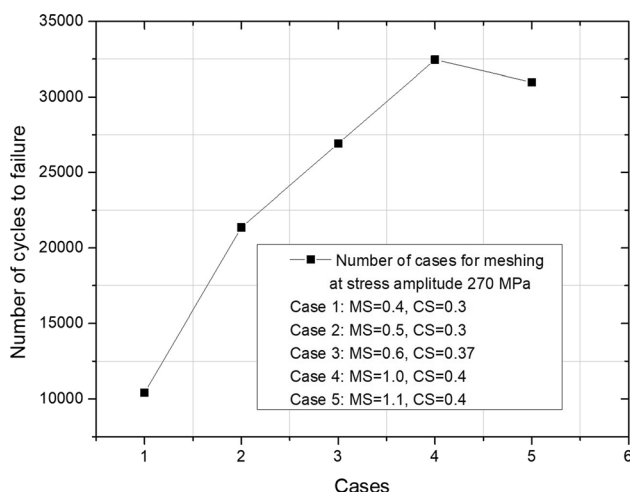


Fig. 4 The grid study of the 3-D finite element analysis model

behavior of change in mesh size with respect to the life cycles of the given material. The optimum mesh size (case 4) MS=1mm, CS=0.4mm has been selected from the grid study as shown in Fig. 4.

Results and Discussion

Microstructure, Plain Fatigue, and Fretting Fatigue Behavior of IMI834 Titanium Alloy

In an optical microscope, the microstructure was observed, and the micrograph of IMI 834 titanium alloy is displayed in Fig. 5, which comprises primary α and transformed β

grains. Both α and β phases were confirmed in this alloy at room temperature. The plain fatigue and fretting fatigue behavior of IMI 834 titanium alloy are demonstrated in Fig. 6. As it is evident from the figure, the fatigue life has been reduced due to the fretting of the bridge-type flat pad with the specimen. The fatigue strength corresponding to 10^6 cycles for plain and fretting fatigue in case of bridge-type flat pad is 280 MPa and 120 MPa. The fatigue strength due to fretting in the case of the bridge-type flat pad is reduced by more than 50% as that of plain fatigue strength. It has been stated that due to the interaction of the contact pad with the specimen, the frictional stress near the contact boundary is high, which causes severe surface loss and results in the decline in fretting fatigue strength [15, 16]. Additionally, from the surface damage observations and FEA results, it is confirmed that the relative slip rises with increasing stress amplitude (Fig. 7) and further leads to an increase in frictional stress near the contact (Fig. 8), which might cause surface loss at the contact surface, which indicates a huge drop in fretting fatigue strength (Tables 3 and 4).

Surface Roughness Measurement and Fracture Surface Observation

Fretting normally occurs by the contact of two mating surfaces, so the surface roughness performs an essential part in the decline of fatigue strength of the material. The surface roughness value is measured in the case of a bridge-type flat pad. The measured average surface roughness value at area no. 1 is $2.7888 \mu\text{m}$ and at area no. 2 is $3.0404 \mu\text{m}$, and the maximum depth in this case (at 270 MPa) is $8 \mu\text{m}$ (at 270 MPa) as shown in Fig. 9. As the stress amplitude decreases, the average surface roughness value decreases from 3.0404 ± 0.3 to $1.892 \pm 0.15 \mu\text{m}$ as shown in Table 5. Earlier researchers studied the crack nucleate near the contact boundary where the stress intensity or frictional stress is high. In this study, the failure takes place at the contact boundary of the specimen where the average surface roughness value is high, which might be due to elevated frictional stress developed. The fretted area under the contact pad in case of bridge-type flat pad (at 270 MPa), which leads to the large surface damage with roughness profiles, is shown in Fig. 9a and b. The high surface roughness value of $3.0404 \mu\text{m}$ near the contact boundary of the pad might be the reason that the crack initiates from the contact boundary of the specimen.

From the fatigue fracture surface, it can be clearly observed that the entire fatigue crack propagation zone is relatively flat and smooth. There are apparently radial

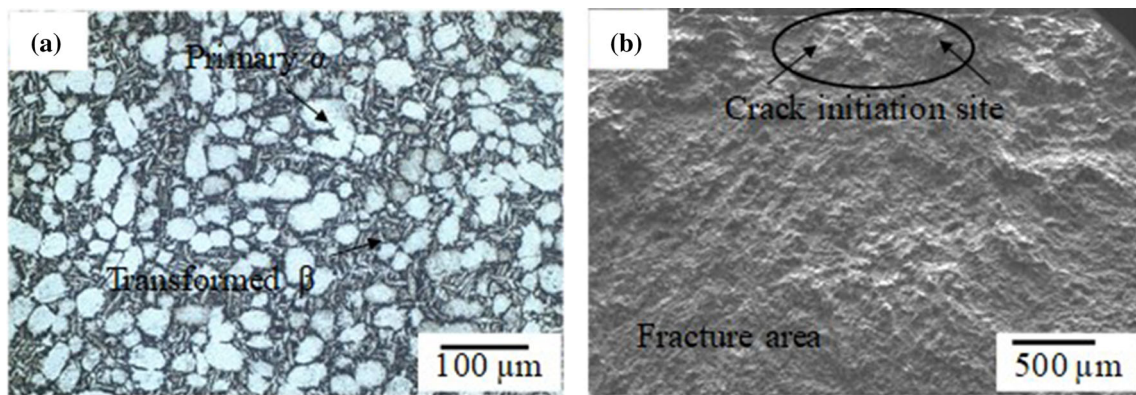


Fig. 5 (a) The optical micrograph of IMI 834 titanium alloy and (b) the fretting fatigue fracture surface

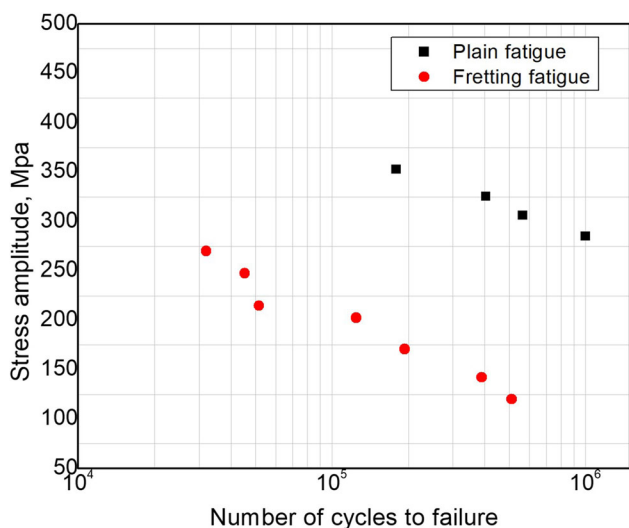


Fig. 6 The S–N curve for plain fatigue and fretting fatigue with bridge-type flat pad

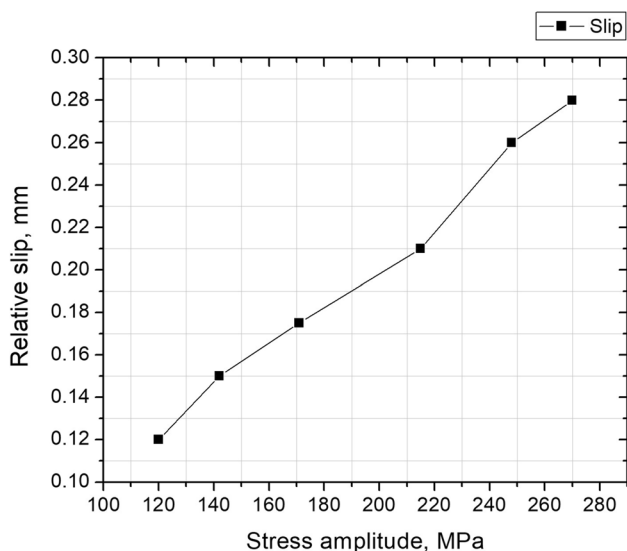


Fig. 7 The relationship between relative slip amplitude with stress amplitude using the FEA model

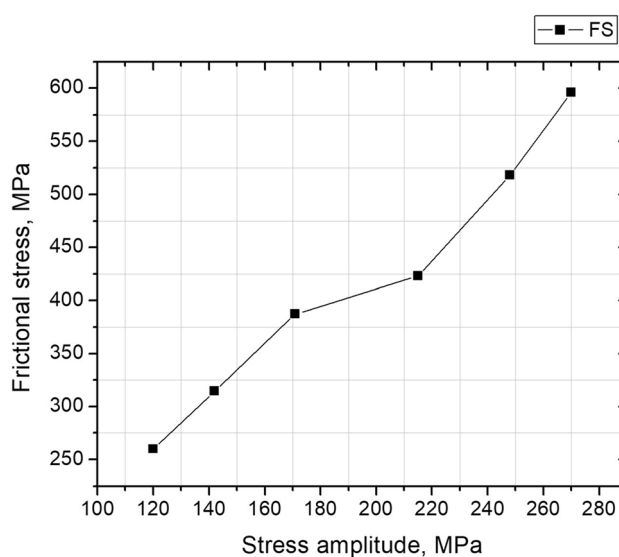


Fig. 8 Relationship between frictional stress with stress amplitude using the FEA model

decorative patterns starting from the crack initiation site, and the crack is originated from the surface of the specimen, which is in contact with the pad. Figure 10 shows magnified images of the fracture surface at 270 MPa, 203 MPa and 120 MPa, which revealed striations in the crack initiation region, and a small number of flat facets appeared indicating by yellow arrows. These facets were formed by the primary α -phase cleavage fracture of the titanium alloy under cyclic loading. The crack initiation and propagation can be divided into three stages [37–40]: (i) stage I (crack initiation or opening stage), crack initiation takes place on a plane inclined about 50 to 60 degrees to the surface in a very early stage of fatigue life, which is mainly controlled by the local contact stresses. (ii) Stage II (crack propagation or shearing stage), a rapid crack propagation will take place during this stage. An oblique crack generated during the propagation and the crack angle depends on the

tangential stress, which is the combination of alternating stress and contact stress. (iii) Stage III (normal crack or tearing stage), there is a change of crack growth direction from oblique to normal because the influence of tangential stress is zero (only alternating stress) as the crack tip moves away from the fretted surface and the final fracture will take place as in plain fatigue. The key variables influencing the fatigue life during fretting are stage I and stage II controlled by the contact stress.

Finite Element Analysis

A detailed study of the process behind the decrease in fatigue strength because of fretting in the case of the bridge-type flat pad was performed by modeling the FEA 3D model. The experimental results were matched with the predicted FEA results as presented in Fig. 11, and it is evident from the images that the experimental values are in good arrangement with the predicted values. The equivalent stress values near the contact pads at stress amplitude of 270 MPa, 203 MPa, and 120 MPa developing FEA 3D model are presented in Fig. 12a, b and c. It has been stated that the stress concentration is closer to the contact boundary [9, 10]. In this work, the high-stress intensity near the boundary of the contact pad (Fig. 13) might result in the generation of crack near the edge, which leads to the failure of the specimen and a large drop in the fatigue strength of the material. The predicted fatigue life at stress amplitude of 270 MPa, 203 MPa, and 120 MPa in the FEA 3D model is presented in Fig. 14a, b and c. These predicted lives were equated with the experimental lives, and it is confirmed that the FEA model results are in good arrangement with the experimental results (Fig. 11).

From the FEA model, the wear rate at stress amplitudes of 270MPa, 248MPa, 215MPa, 203MPa, 171MPa, 148MPa, and 120MPa was also measured by using the Archard equation (Eq 4) to recognize the effect of wear on

Fig. 9 Surface roughness profile on (a) the fretted area no. 1 using coherence scanning interferometer, $S_a = 2.7888 \mu\text{m}$ and (b) the fretted area no. 2 using coherence scanning interferometer, $S_a = 3.0404 \mu\text{m}$

the fretting fatigue behavior of the material. The relationship between wear rate with different stress amplitudes is shown in Fig. 15 as it is clear from the figure; the wear rate rises with increasing stress amplitude values. The wear damage on the surface of the specimen is more because the fretting effect of bridge-type flat pad contact corresponds to the increase in wear loss with stress amplitude, which indicates the decline in the fretting fatigue strength of the material. The wear loss along with the bridge-type flat pad by using FEA model analysis is presented in Fig. 16. From the figure, it is confirmed that the wear loss or wear damage is more near the contact region. This might result in crack formation and a decline in fatigue strength of the material due to fretting.

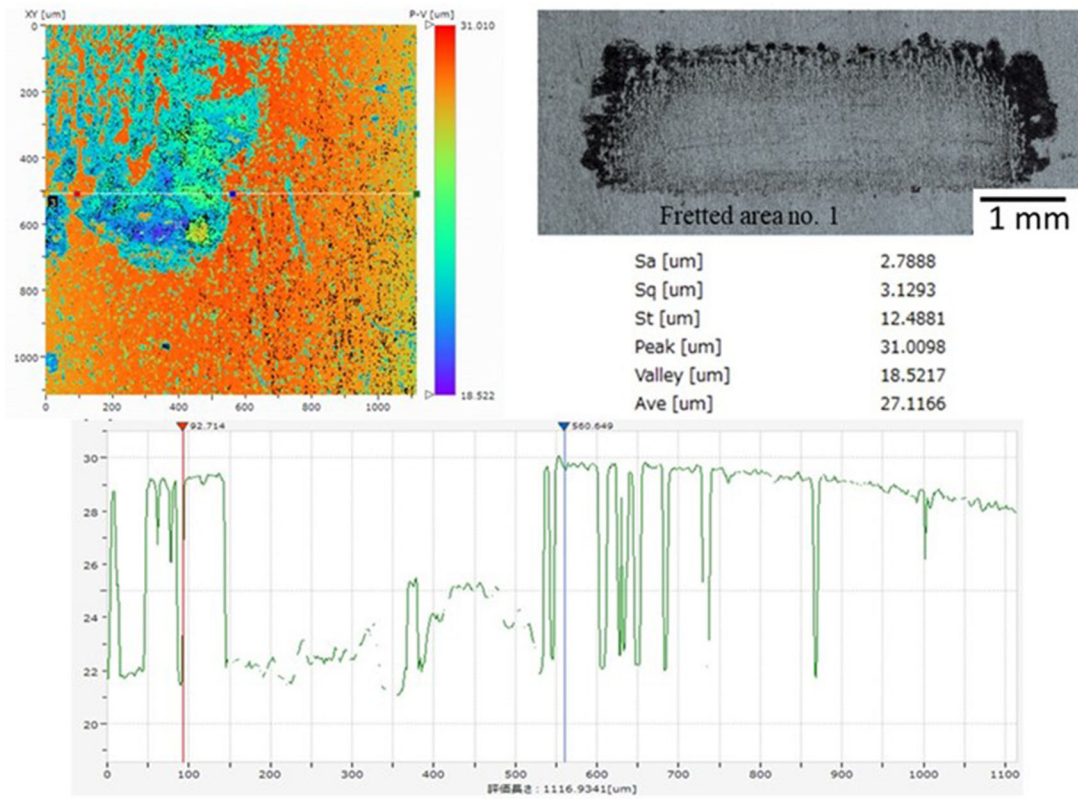
In fretting fatigue conditions, it is necessary to utilize some stress averaging approaches because of the high stress intensity near the interaction region. Many researchers used different stress averaging methods such as point method, line method, volume stress averaging method, and quadrant averaging method to verify the crack origination location and crack angle [27, 28]. In the proposed FEA model, after solving the contact analysis, the line stress averaging method was used to find the crack location and crack angle. In this method, one or two points are taken at the critical damage zone in the predefined outward lines. The value of the Findley parameter is averaged along these lines, the maximum value of the parameter represents the crack origination site, and the line with the greatest parameter is termed as the crack opening angle. The evaluation of crack initiation location and crack angle at stress amplitudes of 270 MPa, 248 MPa,

Table 3 The chemical composition of nickel-based superalloy

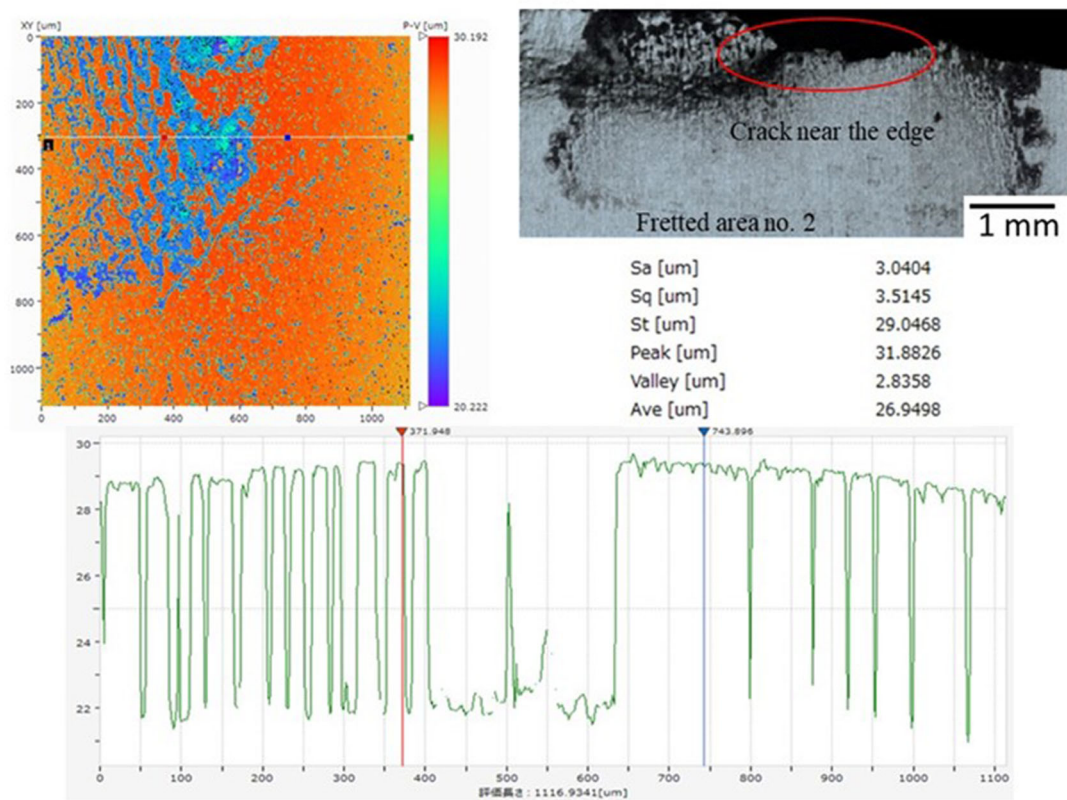
| Chemical composition (wt.%) of Inconel | Cr | Mo | Nb | Fe | Al | Ti | Ta | Si | Co | Mn | C | Ni |
|--|-------|------|------|------|------|-------|--------|------|------|------|-------|------|
| | 20.47 | 8.15 | 3.49 | 0.63 | 0.27 | 0.192 | < 0.05 | 0.04 | 0.03 | 0.01 | 0.019 | Bal. |

Table 4 The mechanical properties of nickel-based superalloy

| Mechanical properties of Inconel | Modulus of elasticity (GPa) | Yield strength (Mpa) | Ultimate tensile strength (Mpa) | Elongation (%) | Density (g/m ³) | Hardness (Hv) |
|----------------------------------|-----------------------------|----------------------|---------------------------------|----------------|-----------------------------|---------------|
| | 205 | 472 | 935 | 40-50 | 8.44 | 210 |



(a)



(b)

215 MPa, 203 MPa, 171 MPa, 148 MPa, and 120 MPa using the line method in the FEA model is presented in Fig. 17. The value of the Findley parameter at stress amplitude of 270 MPa is larger at $\theta = 62$, whereas, in the case of 120 MPa, the value is larger at $\theta = 58$, which represents the crack angle at different stress amplitudes. The influence of stress amplitude values on the fretting fatigue life is demonstrated in Fig. 18. The experimental lives are matched with the predicted FEA lives. It is clear from the co-relation that the experimental results are in excellent arrangement with the predicted FEA results. Two

parallel lines were drawn to evaluate the percentage error in the values. The average percentage error after comparing the results is less than 15%, which is very less as compared to the error reported in the earlier FEA 2D analysis research works [41]. This means that the model developed in this study can be used to understand the stress distribution along the contact region of the component as the model behave very significantly with the experimental fretting fatigue test. The accuracy and reliability of this model were assessed and show that this numerical simulation technique can be used to evaluate crack initiation and stresses distribution between the contact pads. This work is aimed at assessing the accuracy and reliability of the present model based on finite element analysis (FEA) simulations and can be used for different contact shape geometries too.

Table 5 Surface roughness values on fretting scar region of fretting fatigue tested specimen

| Material | Average surface roughness, R_a (μm) of fretted surface | | |
|----------|---|------------------------------|------------------------------|
| | At 270 MPa | At 203 MPa | At 120 MPa |
| IMI834 | $3.0404 \pm 0.3 \mu\text{m}$ | $2.5603 \pm 0.2 \mu\text{m}$ | $1.892 \pm 0.15 \mu\text{m}$ |

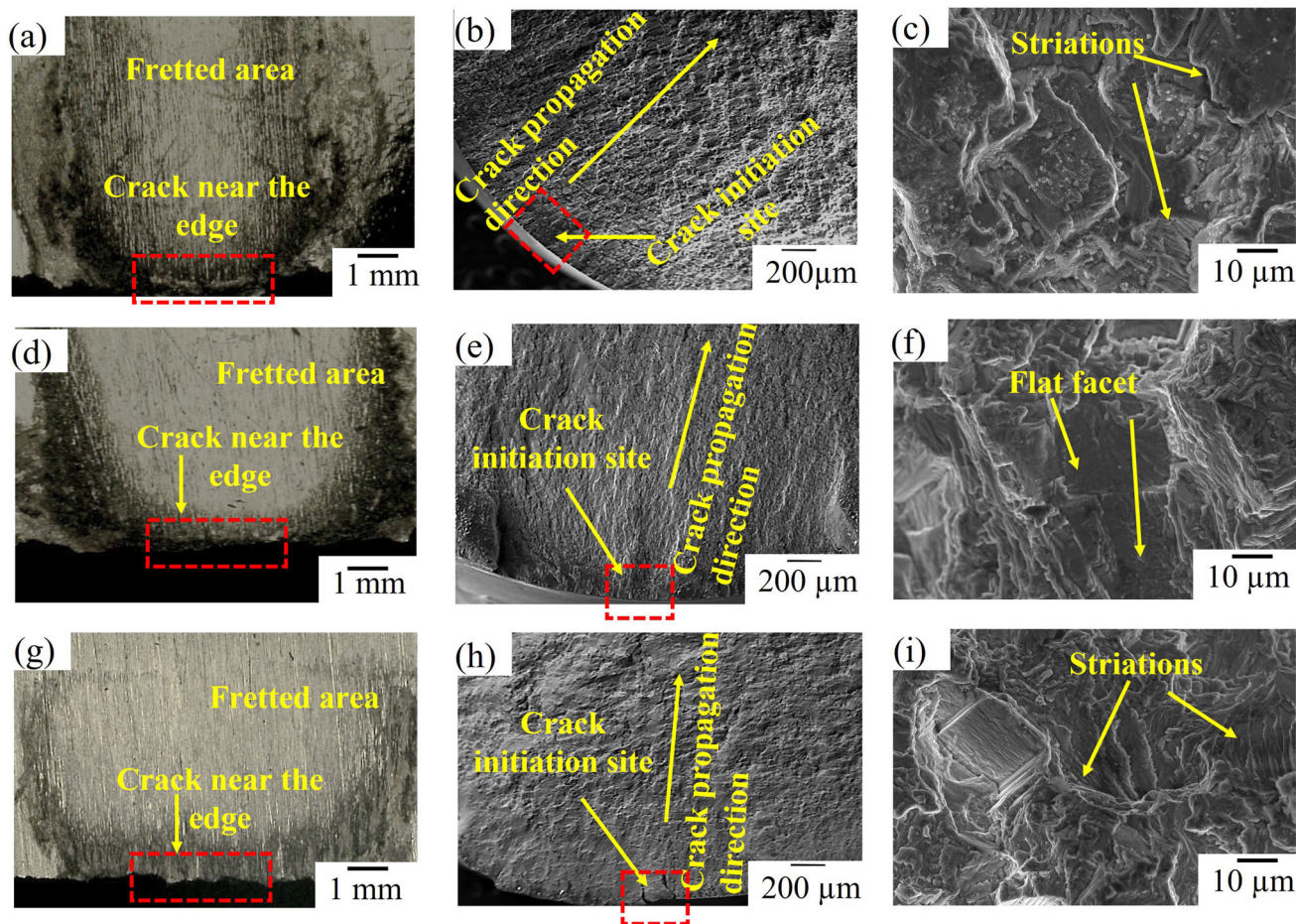


Fig. 10 Fretted surface and fracture surface images at different conditions. (a), (d) and (g) represent fretted surface images at 270 MPa, 203 MPa, and 120 MPa. (b), (e) and (h) represent crack initiation and propagation at 270 MPa, 203 MPa, and 120 MPa. (c),

(f) and (i) represent the highly magnified images with flat facets and striations at 270 MPa, 203 MPa and 120 MPa

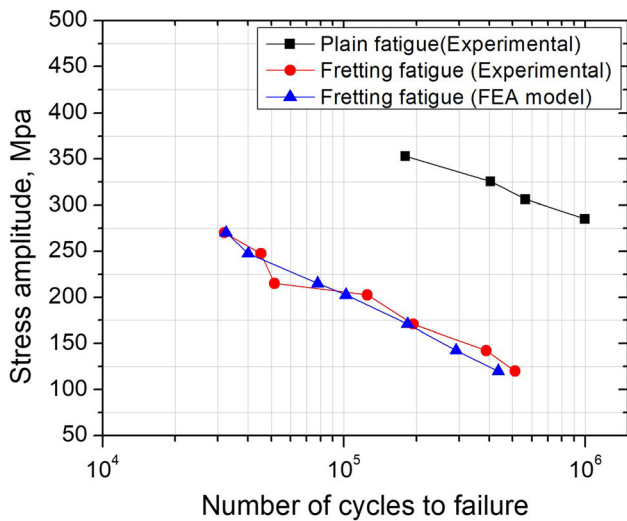


Fig. 11 S–N curve for experimental results vs FEA model results

Conclusions

The FEA 3D model was recommended to identify the damage mechanisms behind the decline in fretting fatigue strength by estimating the performance of stress distribution near the contact sections, crack initiation location, and crack angle. Major conclusions obtained from the obtained results and discussions are summarized as below:

- From experimental results, the fatigue strength was significantly reduced due to the fretting effect of the bridge-type flat pad. The reduction in life might be due to the surface damage that occurs on the smooth surface of the specimen caused by the fretting contact of the pad.
- From the surface damage observations and surface roughness measurement, the damage or failure takes

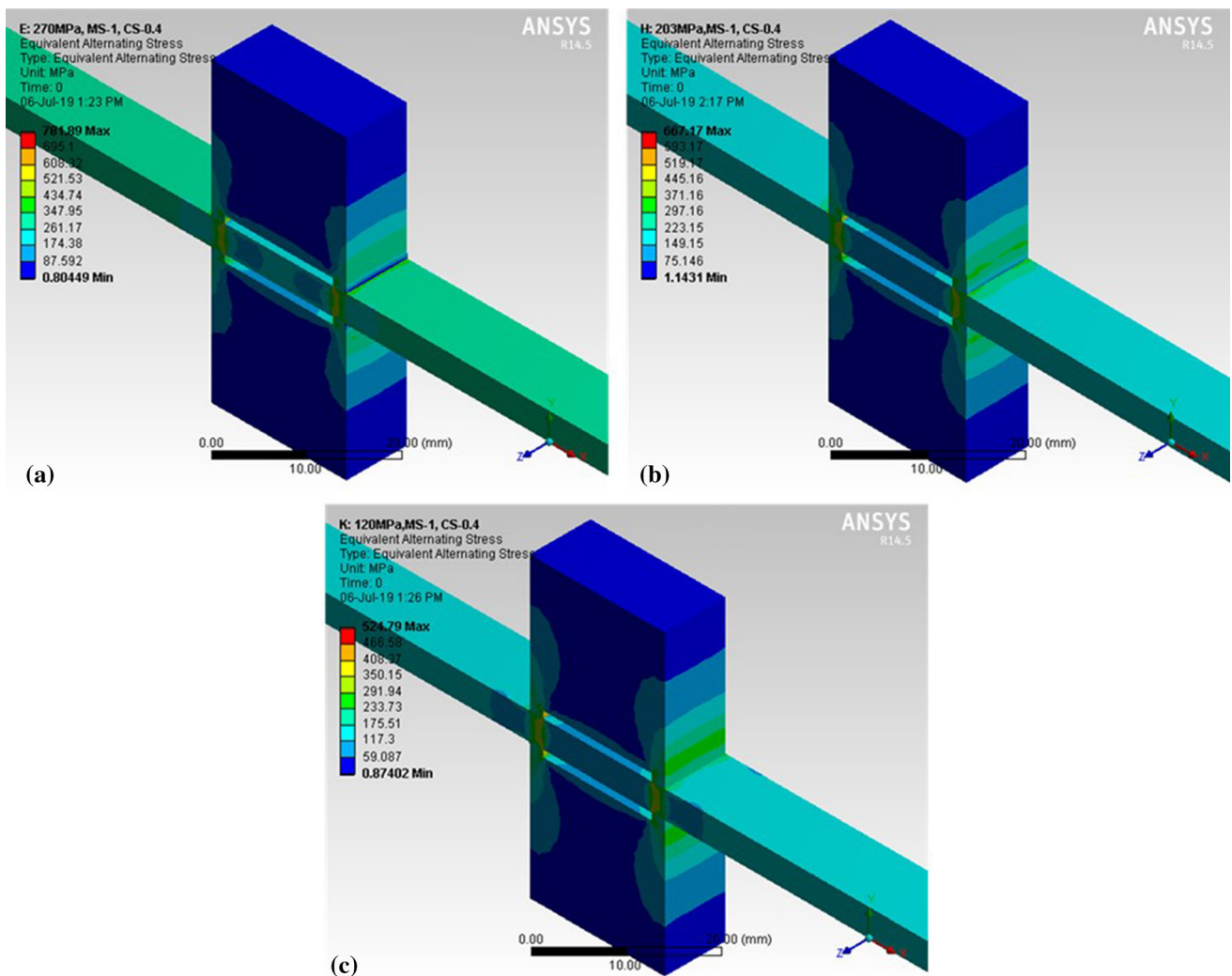


Fig. 12 Equivalent stress distribution along with the contact pads by using the FEA 3D model at different stress amplitudes: (a) at 270 MPa, (b) at 203 MPa, and (c) at 120 MPa

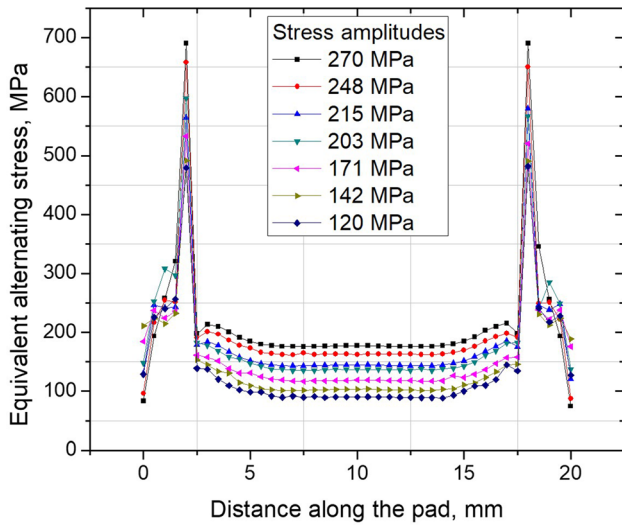


Fig. 13 Stress distribution curve along the contact pad using FEA model

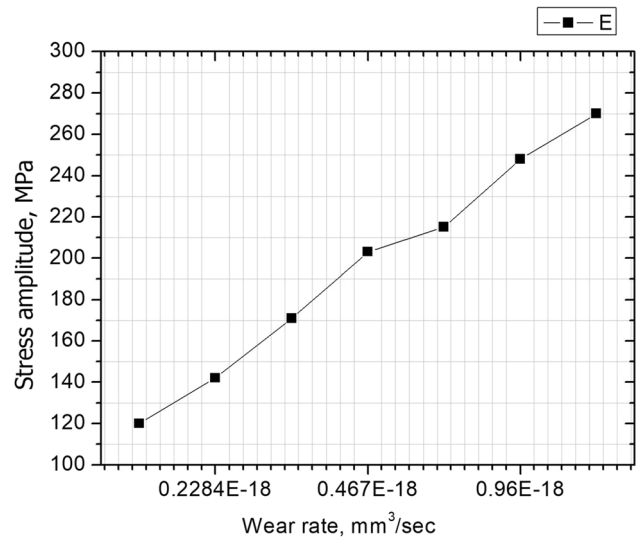


Fig. 15 Wear rate calculation using the FEA model

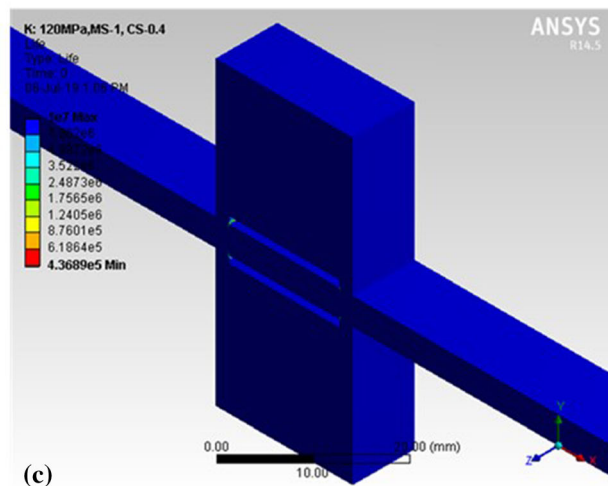
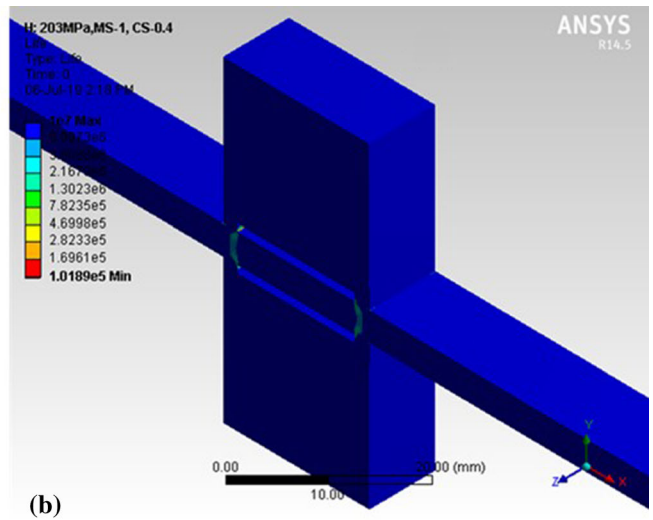
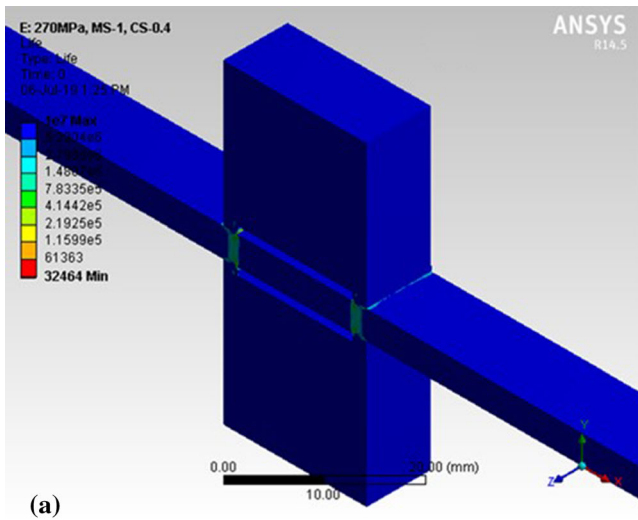


Fig. 14 The fretting fatigue life by using the FEA 3D model at different stress amplitudes: (a) at 270 MPa, (b) at 203 MPa, and (c) at 120 MPa

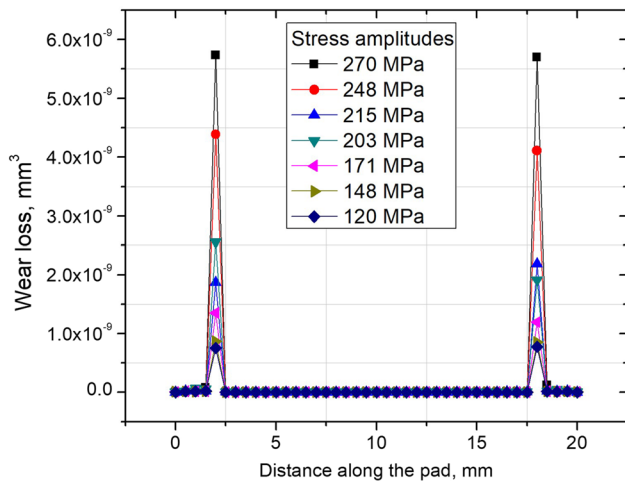


Fig. 16 Wear rate calculation along the contact pad using the FEA model

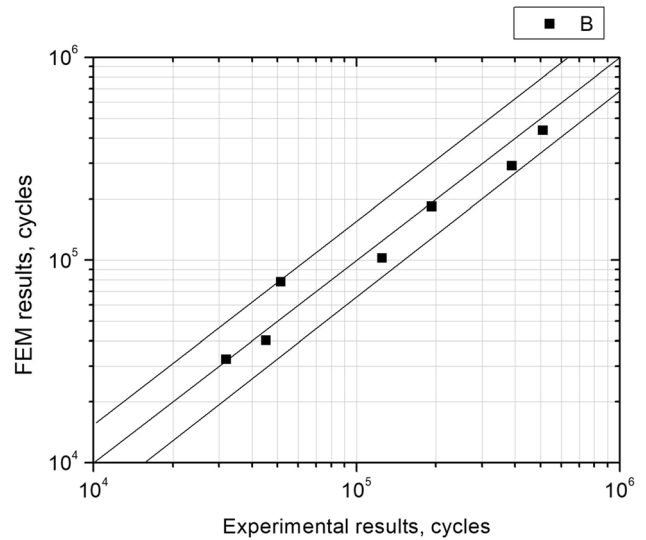


Fig. 18 The co-relation between experimental results and predicted FEA results

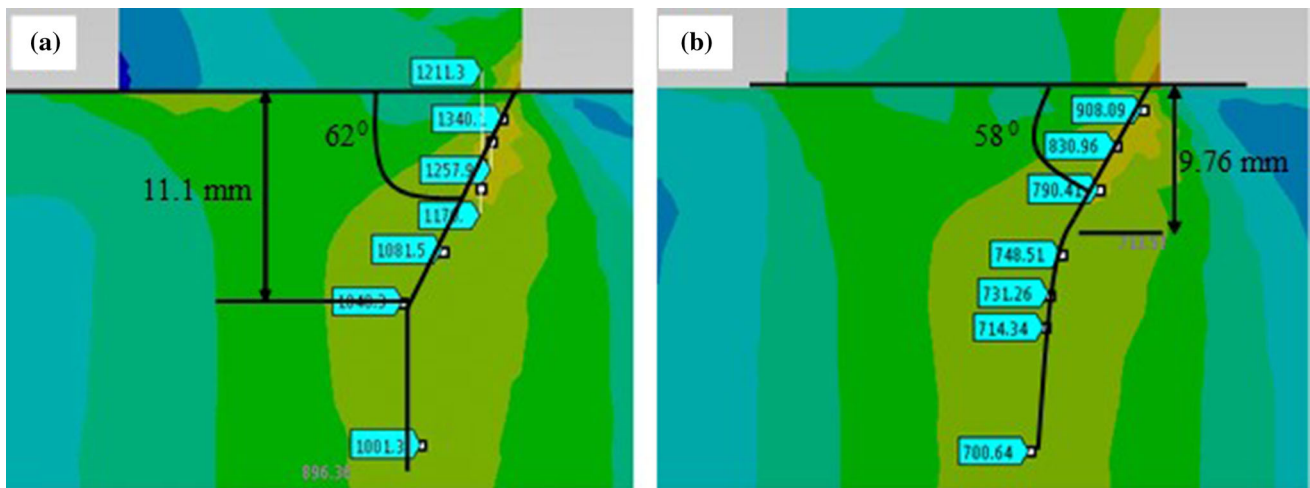


Fig. 17 Crack initiation location and crack angle using the FEA model (a) at 270 MPa and (b) at 120 MPa

place near the contact boundary of the pad, and the average surface roughness value is more near the contact edge, which might be one of the reasons for failure.

- From the proposed FEA model, the experimental results are in good arrangement with the predicted FEA model results. It is confirmed that the relative slip rises with escalating stress amplitude, which causes more frictional stress at the contact. The frictional stress causes more wear loss close to the contact zone, which indicates the decline in fatigue strength due to fretting.
- The critical plane approach is widely accepted to assess the crack initiation site. In these fretting fatigue cases considered, the results reveal that the proposed methodology is also efficient to estimate the fretting fatigue crack initiation location.
- The damage parameter using the stress averaging method was observed. The stress gradient value is high close to the damaged area inside the contact zone, which represents the crack origination location and determines the crack angle using the stress averaging method.

References

- Waterhouse RB, Fretting, Treatise on Materials Science and Technology, 1979; 13: 259–286
- D.A. Hills, D. Nowell, J.J. O'Connor, On the Mechanics of Fretting Fatigue. *Wear*. **125**, 129–146 (1988)
- R.B. Waterhouse, Fretting Wear. *Wear*. **100**, 107–118 (1984)
- Y. Mutoh, Mechanisms of Fretting Fatigue. *JSME Int. J. Series A*. **38**(405), 415 (1995)
- R.B. Waterhouse, Fretting Fatigue. *Int. Mater. Rev.* **37**, 77 (1992)
- R.B. Waterhouse, Fretting at High Temperature. *Tribol. Int.* **14**, 203–207 (1981)
- R.B. Waterhouse, M. Lamb, Fretting Corrosion of Orthopedic Implant Materials by Bone Cement. *Wear*. **60**, 357–368 (1980)
- J.F. Zheng, J. Luo et al., Fretting Wear Behaviors of a Railway Axle Steel. *Tribol. Int.* **43**, 906–911 (2010)
- M. Jayaprakash, Y. Mutoh, K. Yoshii, Fretting Fatigue Behavior and Life Prediction of Automotive Steel Bolted Joint. *Mater. Des.* **32**, 3911–3919 (2011)
- D.G. Wang, M. Abdel Wahab et al., Finite Element Analysis of Fretting Fatigue of Fretted Wires. *Int. J. Fract. Fatigue Wear*. **3**, 135–142 (2015)
- D. Takazaki, M. Kubota et al., Effect of Contact Pressure on Fretting Fatigue Failure of Oil-Well Pipe Material. *Int. J. Fatigue*. (2017). <https://doi.org/10.1016/j.ijfatigue.2017.03.024>
- J. Chao, Fretting-Fatigue Induced Failure of a Connecting Rod. *Eng. Fail. Anal.* **96**, 186–201 (2019)
- R. Garg, G.S. Rao, V. Bhartia, V. Singh, Fretting Fatigue and Wear Behaviour of Timetal 834. *Proc. Eng.* **55**, 661–665 (2013)
- K. Prasad, S. Abhaya, G. Amarendra, V. Kumar, K.V. Rajulapati, K.B.S. Rao, Fatigue crack growth behavior of a near a titanium alloy Timetal 834 at 450 °C and 600 °C. *Eng. Fract. Mech.* **102**, 194–206 (2013)
- M. Jayaprakash, Y. Mutoh et al., Effect of Contact Pad Rigidity on Fretting Fatigue Behavior of NiCrMoV Turbine Steel. *Int. J. Fatigue*. **32**, 1788–1794 (2010)
- Y. Mutoh, M. Jayaprakash, Tangential Stress Range–Compressive Stress Range Diagram for Fretting Fatigue Design Curve. *Tribol. Int.* **44**, 1394–1399 (2011)
- M. Jayaprakash, S. Anchalee, Y. Otsuka, Y. Mutoh, TSR–CSR Diagram for 304 Stainless Steel. *Int. J. Fatigue*. **54**, 99–105 (2013)
- J. Murugesan, Y. Mutoh, Fretting Fatigue Strength Prediction of Dovetail Joint and Bolted Joint by Using the Generalized Tangential Stress Range–Compressive Stress Range Diagram. *Tribol. Int.* **76**, 116–121 (2014)
- N. Noraphaipaksa, C. Kanchanomai, Y. Mutoh, Numerical and Experimental Investigations on Fretting Fatigue: Relative Slip, Crack Path, and Fatigue Life. *Eng. Fract. Mech.* **112–113**, 58–71 (2013)
- N. Noraphaipaksa, A. Manonukul, C. Kanchanomai, Y. Mutoh, Fretting Fatigue Life Prediction of 316L Stainless Steel Based on Elastic–Plastic Fracture Mechanics Approach. *Tribol. Int.* **78**, 84–93 (2014)
- N. Noraphaipaksa, A. Manonukul, C. Kanchanomai, Y. Mutoh, Fretting-Contact-Induced Crack Opening/Closure Behavior in Fretting Fatigue. *Int. J. Fatigue*. **88**, 185–196 (2016)
- A.A. Walvekar, B.D. Leonard, F. Sadeghi, B. Jalalhamadi, N. Bolander, An Experimental Study and Fatigue Damage Model for Fretting Fatigue. *Tribol. Int.* **79**, 183–196 (2014)
- M. Jayaprakash, D. Komatsu, M. Okazaki, Y. Miyashita, Y. Otsuka, Y. Mutoh, High Temperature Fretting Fatigue Behavior of IMI 834 Titanium Alloy. *Trans. Indian Inst. Met.* **69**(2), 439–444 (2016)
- Q.M. Zobaer Shah, M.A. Kowser, M.A. Chowdhury, Investigation of the Combined Effect of Notch and Fretting on Bending Fatigue. *Theor. Appl. Mech.* **47**, 113–122 (2020)
- X. Li, Z. Zuo, W. Qin, A Fretting Related Damage Parameter for Fretting Fatigue Life Prediction. *Int. J. Fatigue*. **73**, 110–118 (2015)
- N.A. Bhatti, M.A. Wahab, Fretting Fatigue Crack Nucleation: A Review. *Tribol. Int.* **121**, 121–138 (2018)
- N.A. Bhatti, K.D. Pereira, M.A. Wahab, Effect of Stress Gradient and Quadrant Averaging on Fretting Fatigue Crack Initiation Angle and Life. *Tribol. Int.* **131**, 212–221 (2019)
- D. Infante-García, E. Giner, H. Miguélez, M.A. Wahab, Numerical Analysis of the Influence of Micro-Voids on Fretting Fatigue Crack Initiation Lifetime. *Tribol. Int.* **135**, 121–129 (2019)
- G. Rousseau, C. Montebello, Y. Guilhem, S. Pommier, A Novel Approach to Model Fretting-Fatigue in Multi-Axial and Non-Proportional Loading Conditions. *Int. J. Fatigue*. **126**, 79–89 (2019)
- W.N. Findley, A Theory for the Effect of Mean Stress on the Fatigue of Metals Under Combined Torsion and Axial Load or Bending. *J. Eng. Ind.* **81**, 301–305 (1959)
- M.P. Szolwinski, N. Thomas, Farris, Mechanics of Fretting Fatigue Crack Formation. *Wear*. **198**, 93–107 (1996)
- K. Pereira, N. Bhatti, M. Abdel Wahab, Prediction of Fretting Fatigue Crack Initiation Location and Direction Using Cohesive Zone Model. *Tribol. Int.* **127**, 245–254 (2018)
- U.B. SumitKhot, Finite Element Analysis of Pin-on-Disc Tribology Test. *Int. J. Sci. Res.* **4**, 1475–1481 (2015)
- M.B. Davanageri, S. Narendranath, R. Kadoli, Finite Element Wear Behaviour Modeling of Super Duplex Stainless Steel AISI 2507 Using Ansys. *Mater. Sci. Eng.* **376**, 1–13 (2018)
- J.M. Thompson, M.K. Thompson, A Proposal for the Calculation of Wear, Mechanical Engineering Dept, MIT
- J.F. Archard, W. Hirst, The Wear of Metals Under Non-Lubricated Conditions. *Math. Phys. Sci.* **236**, 397–410 (1956)
- Q.M.Z. Shah, M.A. Kowser, M.A. Chowdhury, Investigation on the Fretting Fatigue Failure Mechanism of Heat-Treated Al 6061–T6. *Acta Tech. Corviniensis-Bull. Eng.* **12**(3), 119–121 (2019)
- Q.M. Shah, M.A. Chowdhury, M.A. Kowser, Failure Mechanism of Polytetrafluoroethylene Under Friction Fatigue. *J. Fail. Anal. Prev.* **19**(1), 245–249 (2019)
- Q.M. Shah, M.A. Chowdhury, M.A. Kowser, On the Diversity in Design for Different Bending Fretting Fatigue Mechanism. *SN Appl. Sci.* **1**(9), 1–12 (2019)
- M.A. Chowdhury, M.A. Kowser, Q.M. Zobaer Shah, S. Das, Characteristics and Damage Mechanisms of Bending Fretting Fatigue of Materials. *Int. J. Damage Mech.* **27**(4), 453–487 (2018)
- I. Llavori, A. Zabala et al., A Coupled Crack Initiation and Propagation Numerical Procedure for Combined Fretting Wear and Fretting Fatigue Lifetime Assessment. *Theoret. Appl. Fract. Mech.* **101**, 294–305 (2019)

Publisher's Note Springer Nature remains neutral with regard to jurisdictional claims in published maps and institutional affiliations.